Double-Stranded RNA Interacts With Toll-Like Receptor 3 in Driving the Acute Inflammatory Response Following Lung Contusion

Madathilparambil V. Suresh, PhD[1]; Bivin Thomas, MD[1]; David Machado-Aranda, MD[1]; Vladislov A. Dolgachev, PhD[1]; Sadeesh Kumar Ramakrishnan, PhD[2]; Nicholas Talarico, MS[1]; Karen Cavassani, PhD[3]; Matthew A. Sherman, BA[1]; Mark R. Hemmila, MD[1]; Steven L. Kunkel, PhD[3]; Nils G. Walter, PhD[4]; Cory M. Hogaboam, PhD[5]; Krishnan Raghavendran, MD[1]

Objectives: Lung contusion is a major risk factor for the development of acute respiratory distress syndrome. We set to determine the role of toll-like receptor 3 and the binding of double-stranded RNA in the pathogenesis of sterile injury following lung contusion.

Design: Toll-like receptor 3 expression was analyzed in postmortem lung samples from patients with lung contusion. Unilateral lung contusion was induced in toll-like receptor 3 (–/–), TIR-domain-containing adapter-inducing interferon-β (–/–), and wild-type mice. Subsequently, lung injury and inflammation were evaluated. Apoptotic indices, phagocytic activity, and phenotypic characterization of the macrophages were determined. Double-stranded RNA in bronchoalveolar lavage and serum samples following lung contusion was measured. A toll-like receptor 3/double-stranded RNA ligand inhibitor was injected into wild-type mice prior to lung contusion.

Measurements and Main Results: Toll-like receptor 3 expression was higher in patients and wild-type mice with lung contusion. The degree of lung injury, inflammation, and macrophage apoptosis was reduced in toll-like receptor 3 (–/–), TIR-domain-containing adapter-inducing interferon-β (–/–), and wild-type mice with toll-like receptor 3 antibody neutralization. Alveolar macrophages from toll-like receptor 3 (–/–) mice had a lower early apoptotic index, a predominant M2 phenotype and increased surface translocation of toll-like receptor 3 from the endosome to the surface. When compared with viral activation pathways, lung injury in lung contusion demonstrated increased p38 mitogen-activated protein kinases, extracellular signal-regulated kinase 1/2 phosphorylation with inflammasome activation without a corresponding increase in nuclear factor-κB or type-1 interferon production. Additionally, pretreatment with toll-like receptor 3/double-stranded RNA ligand inhibitor led to a reduction in injury, inflammation, and macrophage apoptosis.

Conclusions: We conclude that the interaction of double-stranded RNA from injured cells with toll-like receptor 3 drives the acute inflammatory response following lung contusion. (*Crit Care Med* 2016; 44:e1054–e1066)

Key Words: double-stranded ribonucleic acid; lung contusion; TIR-domain-containing adapter-inducing interferon-β; toll-like receptor 3

Lung contusion (LC) is the primary cause of mortality following blunt chest trauma and blast explosions and is an independent risk factor for the development of acute respiratory distress syndrome (ARDS) and ventilator-associated pneumonia (VAP) (1, 2). It is critical to delineate the factors responsible for the development of progressive respiratory failure as 30% of patients with LC progress to acute lung

[1]Department of Surgery, University of Michigan, Ann Arbor, MI.

[2]Department of Molecular and Integrative Physiology, University of Michigan, Ann Arbor, MI.

[3]Department of Pathology, University of Michigan, Ann Arbor, MI.

[4]Department of Chemistry, University of Michigan, Ann Arbor, MI.

[5]Department of Medicine, Cedar Sinai Medical Center, Los Angeles, CA.

Drs. Suresh and Raghavendran contributed for conception and design. Drs. Suresh, Thomas, Dolgachev, Kumar Ramakrishnan, Talarico, Cavassani, and Mr. Sherman performed research of the article. Drs. Suresh, Machado-Aranda, Hemmila, Kunkel, Hogaboam, and Raghavendran contributed for analysis and interpretation. Drs. Suresh, Walter, and Raghavendran contributed for drafting the article and important intellectual content.

Supported, in part, by National Institutes of Health Grants R01 GM111305-01, HL102013 to Dr. Raghavendran and GM062357 to Dr. Walter.

Dr. Suresh received support for article research from the National Institutes of Health (NIH). Dr. Thomas received support for article research from the NIH. Dr. Ramakrishnan received support for article research from the NIH. Dr. Talarico received support for article research from the NIH, Wellcome Trust/COAF, Howard Hughes Medical Institute (HHMI), Austrian Science Fund (FWF), Bill & Melinda Gates Foundation, World Bank, Research Councils UK (RCUK), and others. Dr. Raghavendran received support for article research from the NIH. The remaining authors have disclosed that they do not have any potential conflicts of interest.

Address requests for reprints to: Krishnan Raghavendran, MD, Professor of Surgery, 1500 E. Medical center drive, 1B407D, UH, University of Michigan, Ann Arbor, MI 48109. E-mail: kraghave@umich.edu

DOI: 10.1097/CCM.0000000000001879

injury/ARDS (1). These conditions have substantial mortality and morbidity, and the resulting economic burden on the healthcare system is considerable.

Toll-like receptors (TLRs) are pattern recognition receptors that recognize exogenous and endogenous molecules released in response to stress, trauma, and cell damage (3). TLR-3 is unique in that it binds a form of nucleic acid called "double-stranded RNA" (dsRNA). Specifically, TLR-3 was initially characterized for its responses to viral dsRNA (4), but more recently, it has been shown that endogenous nucleic acids from necrotic cells activate immune cells through this TLR (5, 6). Although these studies have indicated a role for TLR-3, the precise nature of the ligand and downstream signaling pathways are unclear. Furthermore, the precise role of TLR-3 in LC, bacterial pneumonia, and other nonviral diseases remains largely unknown. Additionally, TLR-3 does not employ the myeloid differentiation primary response gene 88 (MyD88) signaling pathway but instead signals through a unique adaptor protein called "TIR-domain-containing adapter-inducing interferon-β" (TRIF).

In the present study, we examined the role of TLR-3/TRIF and the downstream regulatory pathways in the pathogenesis of acute inflammation and injury in LC. This model reflects a focal, nonlethal disease process that is an independent risk factor for the development of ARDS; importantly, while the model of LC is nonlethal, the pneumonia model is lethal (7, 8). We hypothesized that TLR-3 activation through RNA from necrotic and injured cells may be responsible for driving the acute inflammatory cascade associated with LC. The data presented here indicate that dsRNA released following LC activates the acute inflammatory response, rendering TLR-3 inhibition a potential new therapeutic strategy to limit lung injury.

MATERIALS AND METHODS

Human Lung-Histology and Immunofluorescence Staining

Human LC specimens were obtained from the Heart and Lung Institute, University of British Columbia, Vancouver, Canada, and access to these tissue specimens was approved by the local research ethics committee. For the lung specimens, slides of lung tissue from autopsy samples were obtained from uninjured lung samples and 15 patients who died following LC.

Histology (Human and Mouse Samples)

The formalin-fixed uninjured control and lung-contused sections were paraffin-embedded, sectioned, and stained with hematoxylin and eosin. Histologic findings, such as peribronchial, parenchymal, and perivascular cell infiltration, were semiquantitatively graded in a blinded manner.

TLR-3 Immunofluorescence Staining (Human)

The sections that represented histologic changes consistent with progression of LC in human subjects were further analyzed for immunohistochemical localization of TLR-3. Briefly, 5 μm sections were deparaffinized and rehydrated. Following this, heat-induced epitope retrieval was performed in a decloaking chamber containing 1X citrate buffer-pH-6.0 (Dako, Carpinteria, CA). Sections were washed and blocked (7% bovine serum albumin + 1% fetal calf serum + 0.05% azide) for 15 minutes, incubated overnight at 4°C with polyclonal TLR-3 antibody, and incubated with goat anti-rabbit alexa-594 for 60 minutes at room temperature with intermittent washing. Sections were mounted using ProLong Gold containing 4',6-diamidino-2-phenylindole (DAPI) (Invitrogen, Grand Island, NY). All primary and secondary antibodies were diluted in antibody diluent (Dako) containing 2% normal goat serum (9–11).

TLR-3 Immunofluorescence Staining-Confocal Microscopy

Mouse lung sections were prepared and stained as previously described (8).

Animals

Male (age matched from 6–8 wk) C57BL/6, TLR-3 (–/–), and TRIF (–/–) mice (Jackson Laboratories, Bar Harbor, ME) were used. All procedures performed were approved by the Institutional Animal Care and Use Committee at the University of Michigan and complied with state, federal, and National Institutes of Health regulations.

Murine Model for LC

Male, 20–25 g C57BL/6 (6–8 wk, bred in-house), TLR-3 (–/–), and TRIF (–/–) mice were anesthetized, and LC was induced. Briefly, after induction of anesthesia, each mouse was placed in a left lateral position, and with a cortical contusion impactor, the right chest was struck along the posterior axillary line 1.3 cm above the costal margin with a velocity of 5.8 m/s adjusted to a depth of 10 mm. The mice were then allowed to recover spontaneously.

Albumin Concentrations in Broncheoalveolar Lavage

Albumin concentrations in the broncheoalveolar lavage (BAL) were measured by enzyme-linked immunosorbent assay (ELISA) (Bethyl Laboratories, Montgomery, TX) as previously described (7).

Lung Pressure-Volume (P-V) Mechanics

Pulmonary respiratory mechanics were measured immediately after blood samples were obtained, and the mice were further exsanguinated by transection of the abdominal inferior vena cava. An 18-gauge metallic cannula was inserted into the trachea through a midline cervical exposure. Animals were then connected to a SCIREQ Flexivent (Montreal, QC, Canada) that allows for simultaneous animal ventilation and data capture. Immediate postmortem ventilation was done with the following parameters: tidal volume 10 mL/kg, respiratory rate 150 breaths/min and positive end-expiratory pressure 2 cm H_2O. With PVrV, a controlled inflation and deflation were performed to measure quasi-static compliance values.

Determination of Cytokine Levels in BAL

Interleukin (IL)-1β, macrophage inflammatory protein (MIP)-2, chemokine (C-C) (CCL)-2 (monocyte chemotactic protein

[MCP]-1), CCL-12 (MCP-5), IL-6, keratinocyte chemoattractant (KC), chemokine (C-X-C) (CXC)-10, and tumor necrosis factor (TNF)-α were measured in BAL by ELISA (R&D Systems, Minneapolis, MN) as previously described (7).

Determination of Interferon's Levels in Serum and BAL

Type-1 interferons (α, β) in both serum and BAL samples from TLR-3 (–/–) and wild-type (WT) mice were measured in serum and BAL by ELISA (R&D Systems).

Immunoneutralization of TLR-3 in WT Mice

TLR-3 was blocked by a single injection of monoclonal murine antibodies against this receptor (R&D Systems, Minneapolis, MN). The antibody injections were performed intraperitoneal 48 hours prior to LC (antibody concentration was 20 μg/mouse). The BAL and tissues were harvested at 5, 24, 48, and 72-hour time points. The experimental methodology was similar to the one adapted for the knockout animals.

In Vitro Phagocytosis Assay

Phagocytosis assays were performed as previously described (12). Briefly, after LC in WT and TLR-3 knockout mice, alveolar macrophages (AMs) were isolated from BAL and plated onto a 2×10^5 cells/well and cultured overnight in Dulbecco's Modified Eagle Medium. Wells were aspirated and replaced with 50 μL serum-free medium. Macrophages were then incubated with flouroscein isothiocynate (FITC)-labeled, heat-killed *Pseudomonas aeruginosa*. Phagocytosis of FITC-labeled bacteria was measured after quenching of noningested bacteria with trypan blue.

TaqMan Quantitative Polymerase Chain Reaction

Total RNA was prepared from AMs using RNeasy mini kit, according to the manufacturer's directions (Qiagen, Valencia, CA). A total of 1μg RNA was reverse-transcribed into complementary double-stranded DNA (cDNA) using M-MLV reverse transcriptase (Invitrogen). The cDNA was then amplified by real-time quantitative TaqMan PCR using an ABI Prism 7700 sequence detection system (Applied Biosystems, Foster City, CA). Glyceraldehyde 3-phosphate dehydrogenase was analyzed as an internal control. Taq-Man gene expression reagents or SYBR Green Master PCR mix were used to assay Arginase 1 and Fizz 1 (Applied Biosystems, Grand Island, NY). Data are expressed as fold-change in transcript expression. The fold difference in messenger RNA expression between treatment groups was determined by software developed by Applied Biosystems.

Flow-Cytometry: Apoptosis-Annexin FITC With Annexin V Staining

Apoptosis was performed as previously described (8). Briefly, cells were labeled with Annexin V (BioLegend, San Diego, CA) and incubated for 20 minutes at room temperature. After washing with Annexin V binding buffer, cells were incubated for 10 minutes with LIVE/DEAD stain (Invitrogen, Carlsbad, CA). Cells were washed and blocked with Fc block (CD16/32). The cells were then stained with the following fluorochrome-conjugated mouse antibodies: Ly6C-FITC, Gr-1-phycoerythrin (PE), CD11c-APCCy7, F4/80-AF488, and CD11b-PE-Cy7 (BioLegend and BD Biosciences, San Jose, CA). Data were analyzed using Flow Jo software (Ashland, OR).

TLR-3 Cell-Surface Expression Determination by Flow Cytometry

Intracellular and extracellular TLR-3 expression was determined using flow cytometry. BAL macrophages were obtained from uninjured control and WT mice after LC. Fc binding was blocked with anti-mouse CD16/32 antibody, and the cells were incubated with PE-conjugated anti-F4/80 and pacific blue conjugated anti-CD45 antibody (BioLegend, San Diego, CA). The cells were then fixed, permeabilized, incubated with polyclonal rabbit anti-mouse TLR-3 antibody or rabbit immunoglobulin G (IgG), and stained with FITC-conjugated anti-rabbit IgG. The cells were not permeabilized for extracellular staining of TLR-3. Data were analyzed using Flow Jo software.

MyD88 Staining and Flow Cytometry

BAL cells were collected after LC. The cells were fixed, permeabilized, and subjected to intracellular staining. The following primary antibodies were used; MyD88 (R&D system, Minneapolis, MN) CD11c-FITC, TLR-3-PE, and F4/80-APC-Cy7 (BioLegend, San Diego, CA). Data were analyzed using Flow Jo software.

Preparation and Isolation of RNA From Necrotic Cells and Coculture With AMs

RNA was isolated from BAL of WT mice 24 hours following LC. AMs from TLR-3 (–/–) and WT mice were harvested from the BAL of uninjured animals. These macrophages were cocultured in the presence of RNA. At 24 hours, the medium was collected and measured for proinflammatory cytokines by ELISA.

Western Blots

Western blots were performed as previously described (12) (All antibodies from Cell Signaling Technology, Beverly, MA).

RNA Analysis by Nondenaturing Polyacrylamide Gel Electrophoresis

To investigate the presence of dsRNA in BAL and serum samples following LC, nondenaturing polyacrylamide gel electrophoresis was performed. The total RNA (50 μg) of the samples and the dsRNA marker (Abnova, Walnut, CA) were electrophoresed on a 7.5% nondenaturing polyacrylamide gel at 200 V in a 4°C cold room. The gel was run at 18 W for 2–3 hours. After electrophoresis, the gel was stained; RNA was identified.

dsRNA Immunocytochemistry

AMs were fixed by adding formaldehyde directly to the cells for 15 minutes at room temperature. Cells were washed with phosphate-buffered saline (PBS), permeabilized with 0.2% Triton X-100 (Sigma-Aldrich, St. Louis, MO), washed twice with PBS, and blocked with PBS containing 1% bovine serum albumin (BSA). MabJ2, which was obtained from English & Scientific Consulting (Szirák, Hungary), was used to detect dsRNA, and monoclonal

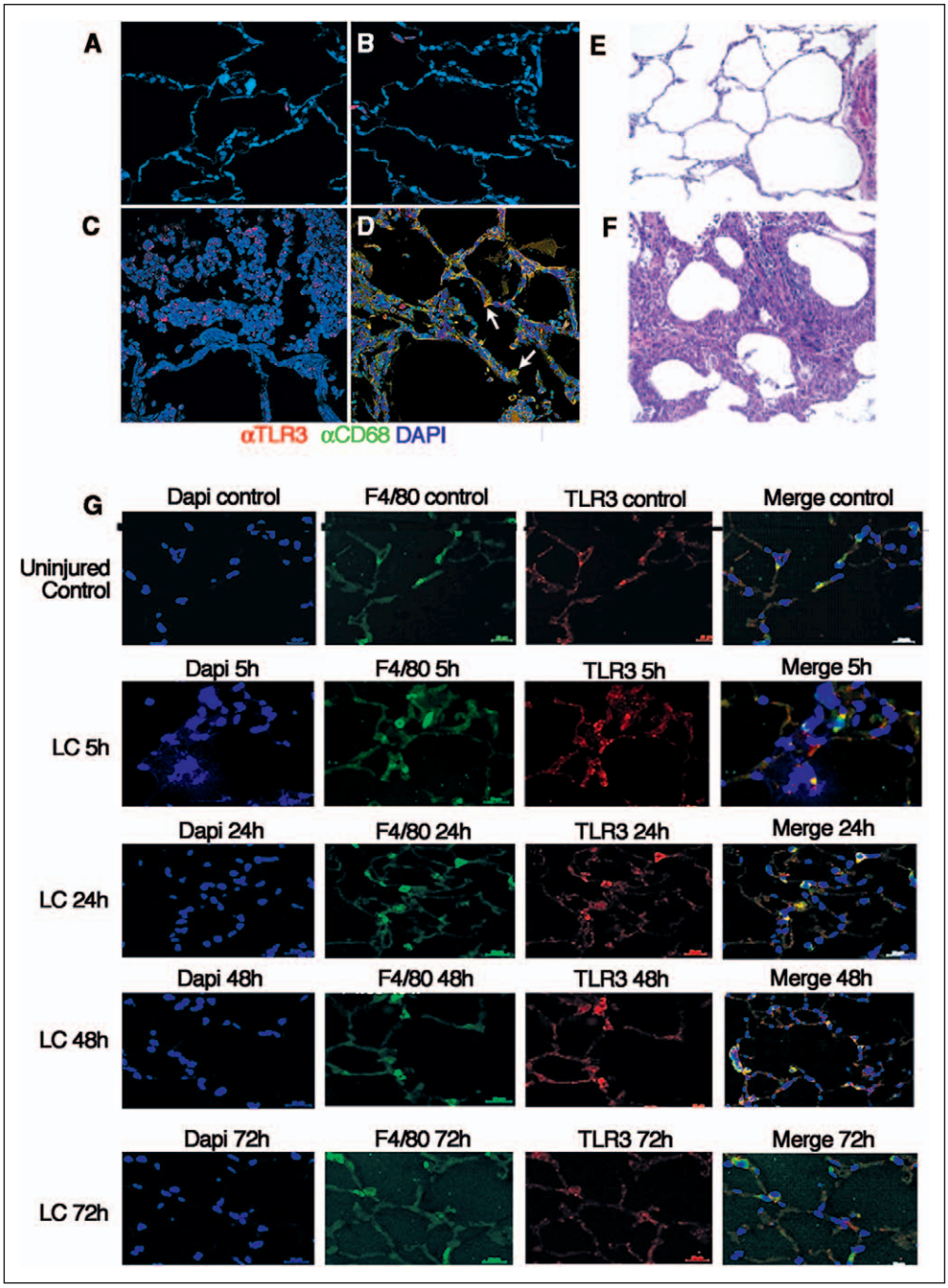

Figure 1. Increased toll-like receptor (TLR) 3 expression in lung contusion (LC). Postmortem lung samples in patients with LC compared to normal lung tissue. Representative confocal images from normal human lung (**A**), normal lung stained with anti-TLR-3 antibody (**B**), lung with LC stained with anti-TLR-3 antibody (*red*) (**C**), and LC-colocalization with antibodies to TLR-3 and cluster of differentiation 68 (CD68) alveolar macrophages (*green*) (**D**). Histological analysis of postmortem lung samples in control (**E**) and patient with LC (**F**). These samples were obtained from the tissue bank at the University of British Columbia. No clinical data correlates other than the diagnosis of the banked specimen was provided. **G**, Wild-type (WT) mice showed predominant TLR-3 expression following LC. WT mice on C57BL/6 background were subjected to LC. The lung samples were harvested at 5, 24, 48, and 72 hr time points, and the samples were subjected to immunofluorescent staining with F4/80 for macrophages (*green*), TLR-3 (*red*), and nuclear staining with 4',6-diamidino-2-phenylindole (DAPI) ($n = 3$ per group). Overlay composite view is provided.

anti-TLR-3 polyclonal antibody was used to detect TLR-3. Fixed and permeabilized cells were incubated overnight at 4°C with diluted MabJ2 in PBS/1% BSA (1:500 dilution of the 0.200 mg/mL antibody). Cells were washed twice with PBS and incubated with Alexa-fluor labelled secondary antibodies (Invitrogen) for 1 hour. Nuclei were stained with DAPI, the cells on coverslips were mounted in mounting media (Dako), and photomicrographs of the invasive sections were analyzed digitally using Photoshop software version 9.0.2 (San Jose, CA).

Ribonuclease Treatments

The ribonuclease (RNAase) III (Invitrogen) and RNase A were purchased from Sigma-Aldrich. For dsRNA staining, macrophages were collected after LC, fixed, permeabilized as described above, and incubated for 2 hours at 37°C with RNase III (2 μg/mL) in reaction buffer or with RNase A (1 μg/mL) in PBS. After the incubation period, cells were washed 10 times with washing buffer and processed for immunofluorescence as described above.

Intracellular dsRNA Staining and Flow Cytometry

For the detection of intracellular staining for dsRNA, BAL cells were collected after LC. The cells were fixed, permeabilized, and subjected to intracellular staining (13). The following primary antibodies were used: J2 (English & Scientific Consulting), CD11c-FITC, and F4/80-APC-Cy7 (BioLegend, San Diego, CA) (14). Data were analyzed using Flow Jo software.

TLR-3/dsRNA Complex Inhibitor Administration (In Vivo)

The TLR-3/dsRNA complex inhibitor ((R)-2-(3-Chloro-6-fluorobenzo [b] thiophene-2-carboxamido)-3-phenylpropanoic acid, Calbiochem/EMD Millipore, Billerica, MA) was dissolved in dimethyl sulfoxide and diluted in sterile PBS. The inhibitor (1 mg per mouse) (15) was administered (intraperitoneal) into the mice 2 hours before LC. Mice were subjected to treatment (intraperitoneal)

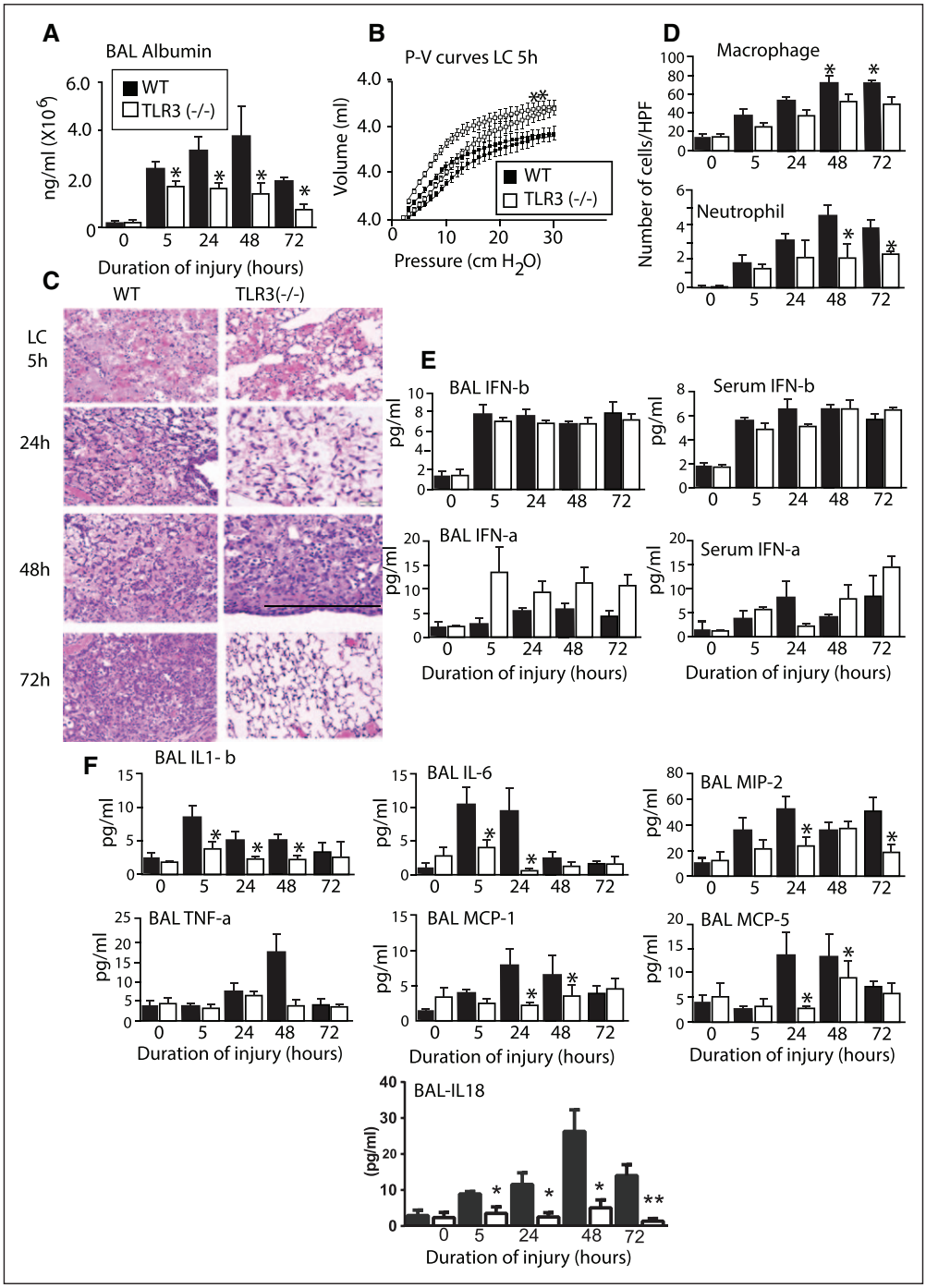

Figure 2. Injury and inflammation were reduced in toll-like receptor (TLR) 3 (−/−) mice following lung contusion (LC). **A**, After LC, mice were killed at different time points, and albumin concentration in the broncheoalveolar lavage (BAL) was determined by enzyme-linked immunosorbent assay (ELISA) ($n = 16$ per group). **B**, Pulmonary compliance measurements in wild-type (WT) and TLR-3 (−/−) mice following LC. "Quasi-static" closed chest pressure-volume (P-V) behavior was measured at 5 hr postinjury in WT and TLR-3 (−/−) mice. The total lung capacity was higher in the TLR-3 (−/−) mice. $^{**}p < 0.05$ WT versus TLR-3 (−/−) mice. **C**, Histological evaluation of TLR-3 (−/−) mice following LC: In WT mice, there were large areas of hemorrhage at 5 hr with increasing necrosis and inflammation at 24 and 48 hr compared to TLR-3 (−/−) mice. Unlike the WT, TLR-3 mice showed resolution by 72 hr. **D**, Macrophage and neutrophil levels in BAL were higher in WT mice following LC. Cytospin analysis of BAL samples was performed after lung injury. The levels of macrophages and neutrophils were significantly higher at all-time points in WT mice compared to TLR-3 (−/−) mice ($n = 16$ per group). **E**, Increased inflammatory response in WT was not associated with differences in levels of type-1 interferons (IFNs). BAL IFN β, serum IFN β, BAL IFN α, and serum IFN α were measured by ELISA ($n = 6$ per group). **F**, TLR-3 (−/−) mice showed a significant reduction in cytokine response compared to WT following LC: The levels of interleukin (IL)-6, IL-1β, macrophage inflammatory protein (MIP)-2, tumor necrosis factor (TNF)-α, monocyte chemotactic protein (MCP)-5 (chemokine (C-C) [CCL]12), MCP-1 (CCL2), and IL-18 in the BAL were significantly higher in WT mice following LC compared to TLR-3 (−/−) mice ($n = 16$). Statistical analysis was performed with two-tailed unpaired *t* test with Welch correction. $^{*}p < 0.05$ WT versus TLR-3 (−/−) mice.

with polyinosinic:polycytidylic acid (poly I:C) (20 mg/kg body weight) (Sigma Aldrich) 1 hour before LC.

TLR-3/dsRNA Complex Inhibitor Administration (Ex Vivo)

AMs of WT mice were harvested from the BAL 24 and 48 hours following LC. These macrophages were cocultured in the presence of necrotic RNA (24 hr after LC), TLR-3/dsRNA inhibitor (27 μm/mL), and/or the synthetic dsRNA molecule poly-I:C (10 μg/mL). The medium was collected after treatments and measured for proinflammatory cytokines by ELISA.

ApoStat

Intracellular caspase activity was measured by ApoStat (R&D Systems). BAL cells were washed and fixed with 1% formalin and reconstituted in 300 μL of flow buffer. Intracellular caspase activity was measured by an ApoStat kit (R&D Systems) as described by the manufacturer's protocol.

Statistical Methods

Data are expressed as mean ± SEM. Statistical significance was estimated using one-way analysis of variance. Individual intergroup comparisons were analyzed using two-tailed, unpaired *t* test with Welch correction (Graph Pad Prism 6.01, La Jolla, CA). Significance was set at *p* value less than or equal to 0.05.

RESULTS

Human and Mouse LC Samples Show High Expression of TLR-3

Intense TLR-3 Staining of AMs and Epithelial Cells in Postmortem Human Lungs. Histopathologic evaluation of postmortem samples from

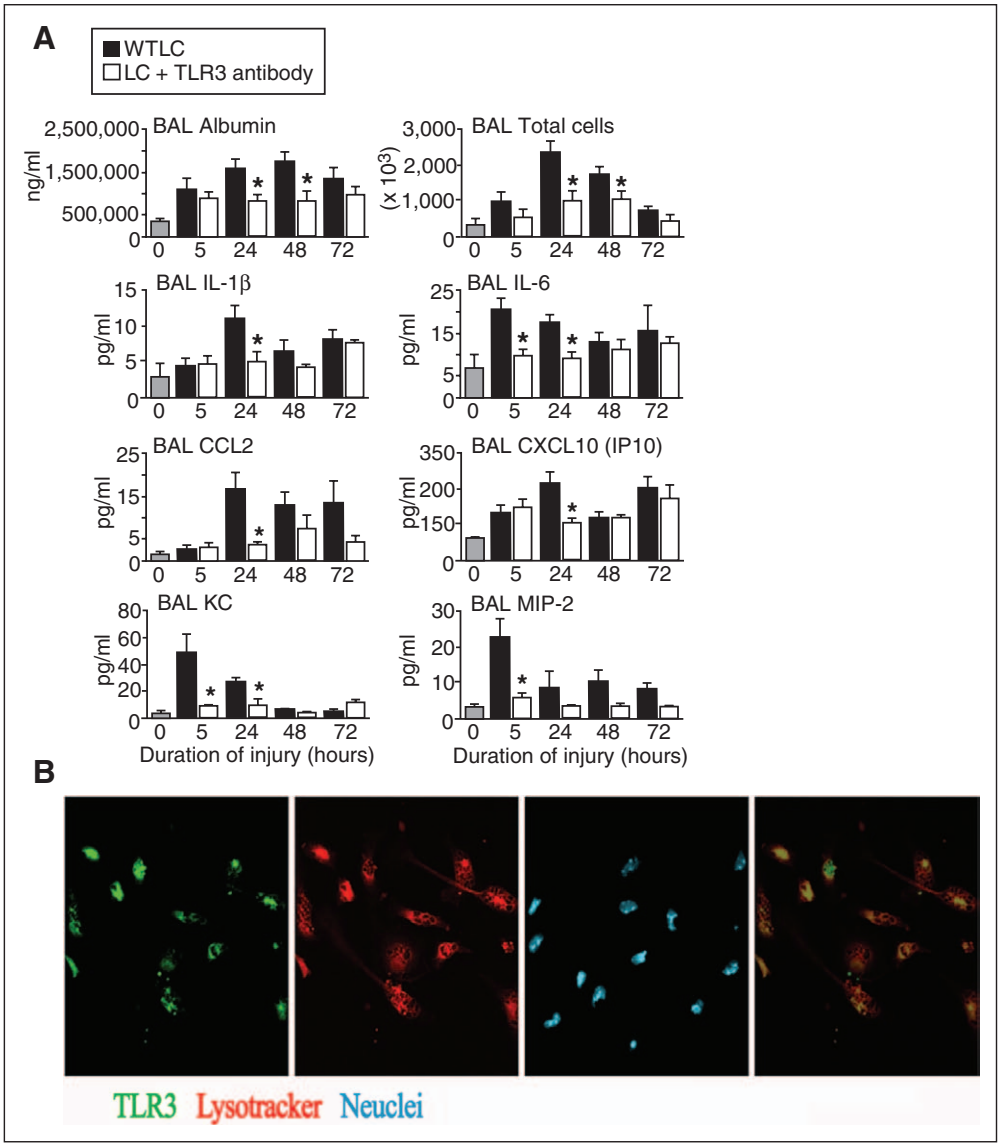

Figure 3. Functional importance of toll-like receptor (TLR) 3 using antibody neutralization in the development of lung injury following lung contusion (LC). **A**, Monoclonal murine antibodies to TLR-3 (or saline and immunoglobulin G [IgG] for controls) were administered IP 48 hr prior to LC in wild-type (WT) animals. Values with IgG controls were similar to saline and have been omitted for clarity. Albumin, which is representative of permeability injury, and total cells in the broncheoalveolar lavage (BAL) fluid were quantified as described in the *Materials and Methods* section. Interleukin (IL)-1β, IL-6, monocyte chemotactic protein (MCP)-1, chemokine (C-X-C) (CXC) (CXCL) 10, keratinocyte chemoattractant (KC), and macrophage inflammatory protein (MIP)-2 levels in the BAL of WT and TLR-3 (–/–) mice were analyzed by enzyme-linked immunosorbent assay after injury ($n = 6$). The total number of macrophages was higher in WT mice compared to the anti-TLR-3 antibody-administered groups (data not shown). The wild type mice treated with anti-TLR-3 antibody exhibited significantly less acute neutrophil recruitment at 48 hr in response to LC (data not shown). There was no significant difference in the levels of IL-1β between the two groups at 5 hr after LC, but there was a significant decrease in IL-1β levels at the 24 hr time points in the antibody administered mice compared to the corresponding control. The levels of the cytokines IL-6, MCP-1, CXCL-10, KC, and MIP-2 were lower in the mice treated with anti-TLR-3 antibody compared to corresponding control groups. $^*p < 0.05$ WT versus corresponding antibody treated mice. **B**, To confirm the intracellular entry of the antibodies, the macrophages were costained with anti-TLR-3 antibody and Lysotracker (lysosomal staining). The overlay composite view is provided. CCL = chemokine (C-C).

patients with LC reveals a significant degree of severe diffuse alveolitis characterized by influx of macrophages, and rare lymphocytes were seen compared to the normal lungs. Immunofluorescence data demonstrated that the samples from patients with LC have significant expression of TLR-3, especially in the alveolar lining and macrophages (**Fig. 1**, ***A–F***).

AM and Epithelial Cells Show High Expression of TLR-3 in Mice Following LC. Immunofluorescent images show intense TLR-3 signal in AMs and epithelial cells (**Fig. 1*G***).

TLR-3 Is Functionally Important in the Development of Progressive Lung Injury Following LC

TLR-3 (–/–) Mice Exhibited Decreased Permeability Injury and Inflammation With LC. We have previously shown that the acute inflammatory response in LC is responsible for deficits in oxygenation and increases in quasi-static pulmonary compliance and severe permeability injury (BAL albumin) (8, 16–19). While there was a significant decrease in the BAL albumin level in TLR-3 (–/–) mice (**Fig. 2*A***), pulmonary compliance and volumes were significantly lower in WT mice (**Fig. 2*B***). Histologic evaluation of WT mice showed significantly more injury than TLR-3 (–/–) mice at all-time points (**Fig. 2*C***). The numbers of macrophages/neutrophils (**Fig. 2*D***) and levels of proinflammatory cytokines (IL-1β, IL-18, and IL-6), chemokines MCP-1 and MCP-5, and MIP-2 were uniformly higher in WT mice (**Fig. 2*F***). These molecules reflect the various attributes of acute and sub-acute inflammatory response following LC (16, 20).

TLR-3 Driven Inflammatory Response Is Not Mediated by Type-1 Interferons. In additional experiments, the difference in the elaboration of type-1 interferons (α, β) in both serum and BAL samples from TLR-3 (–/–) and WT mice yielded low levels with very little difference (**Fig. 2*E***). Measurements of transcript levels of type-1 IFNs in AMs were elevated at 2 hours following LC in WT mice, but these levels returned to those seen in uninjured mice by 24 hours (data not shown). These results indicate that pathways

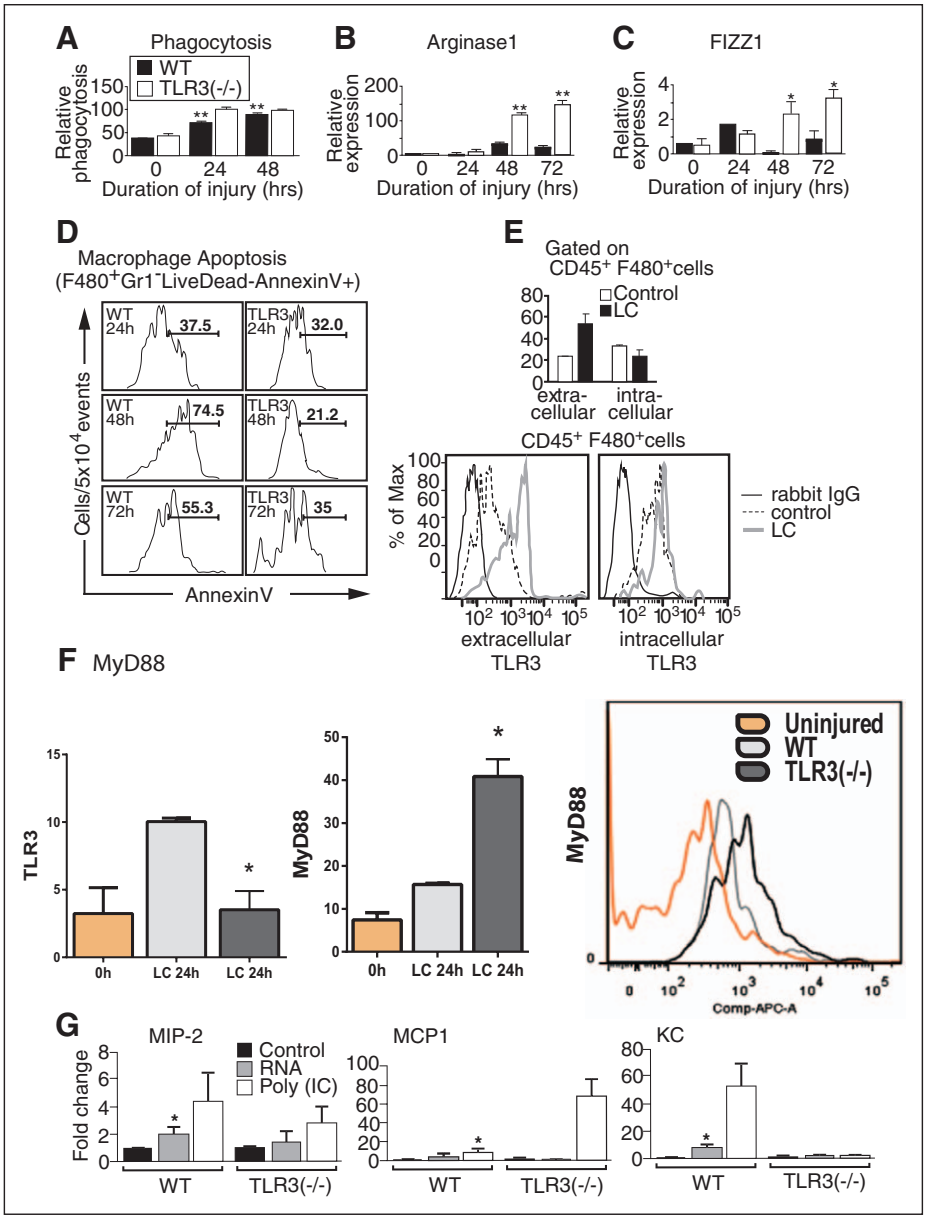

Figure 4. Phenotypic alteration, characterization, localization of the receptor, and cytokine production of alveolar macrophage following lung contusion (LC). Phagocytosis assay **A**, Broncheoalveolar lavage (BAL) macrophages from wild-type (WT) and toll-like receptor (TLR) 3 (–/–) following LC were incubated with flouroscein isothiocynate-labeled heat-killed *Pseudomonas aeruginosa* ($n = 6$). Quantitative TaqMan polymerase chain reaction analysis: Arginase-1 (**B**) and "FIZZ1" (**C**) transcript expression were measured in WT and TLR-3 (–/–) mice following LC. Real time PCR analysis showed there was a significant increase in the levels of Arginase-1 and Fizz-1, the classic M2 marker genes, at 48 and 72 hr in TLR-3 (–/–) mice ($n = 5$). $^{**}p < 0.01$ and $^{*}p < 0.05$ WT versus TLR-3 (–/–). **D**, TLR-3 (–/–) mice show reduced apoptosis of alveolar macrophage compared to WT following LC. The BAL cells were stained with fluorochrome-conjugated mouse antibodies. Macrophages and neutrophils were selected for fluorescence-activated cell sorting scan analysis. The figure shown here reflects values from a single animal in each group. Values are represented as mean ($n = 6$ per group). $^{*}p < 0.05$ versus TLR-3 (–/–) mice. **E**, TLR-3 expression in BAL macrophages. Immunofluorescence analyses of TLR-3 in macrophages were performed. For intracellular staining, cells were fixed and permeabilized and subsequently incubated with anti-TLR-3 Ab. For cell surface staining, cells were fixed and incubated with anti-TLR-3 Ab. ($n = 3$). **F**, Myeloid differentiation primary response gene 88 (Myd88) expression in BAL macrophages. Flow cytometry analyses of TLR-3 and MyD88 in macrophages were performed. For staining, cells were fixed and permeabilized and subsequently incubated with anti MyD88 and anti-TLR-3 Ab. ($n = 3$). **G**, RNA from alveolar macrophages following LC induced more cytokine production in WT mice than TLR-3 (–/–) mice. RNA isolated from alveolar macrophages after LC was cocultured with uninjured WT and TLR-3 (–/–) mice alveolar macrophages respectively in the presence or absence of Poly:immune complex (IC). The cell culture media collected and the levels of proinflammatory mediators macrophage inflammatory protein (MIP)-2, keratinocyte chemoattractant (KC), and monocyte chemotactic protein (MCP)-1 were measured ($n = 6$ per group). $^{*}p < 0.05$ WT mice versus corresponding TLR-3 (–/–) group. CD = cluster of differentiation, IgG = immunoglobulin G.

other than type-1 IFNs are implicated in the TLR-3-driven pathogenesis of inflammation in LC.

Additional experiments were performed by administering mouse monoclonal antibody to TLR-3 48 hours prior to LC in C57BL/6 mice using IgG and saline control mice ($n = 6$). Consistent with the results from TLR-3 (–/–) mice studies, the degree of injury and inflammation (albumin and BAL cells/cytokines levels) was consistently lower with the administration of monoclonal antibody against TLR-3 (**Fig. 3*A***). Additionally, we were able to document the intracellular entry of these antibodies (**Fig. 3*B***). Taken together, these data demonstrate that the absence of TLR-3 confers a protective role as evidenced by the decrease in not only lung permeability injury but also the acute inflammatory response to LC. We conclude that TLR-3 plays a role in up-regulating the intensity of acute inflammation following LC.

Alteration of AM* Phenotype, Phagocytic Activity, Apoptosis, *and* Generation *of* Inflammatory Cytokines *in LC* Is Dependent *on TLR-3*.** Macrophage phenotypes can be characterized as proinflammatory (M1) or immunomodulatory and tissue remodeling (M2). Macrophage polarization into M1 or M2 phenotype dictates the nature, duration, and severity of an inflammatory response (7, 21). Since increased susceptibility to bacterial infection during lung injury correlates with defects in AM phagocytosis, we measured ex vivo phagocytosis in an in vitro assay using isolated AMs from wild type and TLR-3 (–/–) mice. The relative phagocytic activity was significantly higher after LC in the TLR-3 (–/–) mice at 24 and 48-hour time points (**Fig. 4*A). The M1 phenotype (also termed as classically activated) is characterized by increased production of oxidative burst and nitric oxide release. Unmitigated expression of M1 phenotype indicates significant injury, particularly in sterile injury, such as LC. Conversely, the M2 phenotype (also termed as alternatively activated) is associated

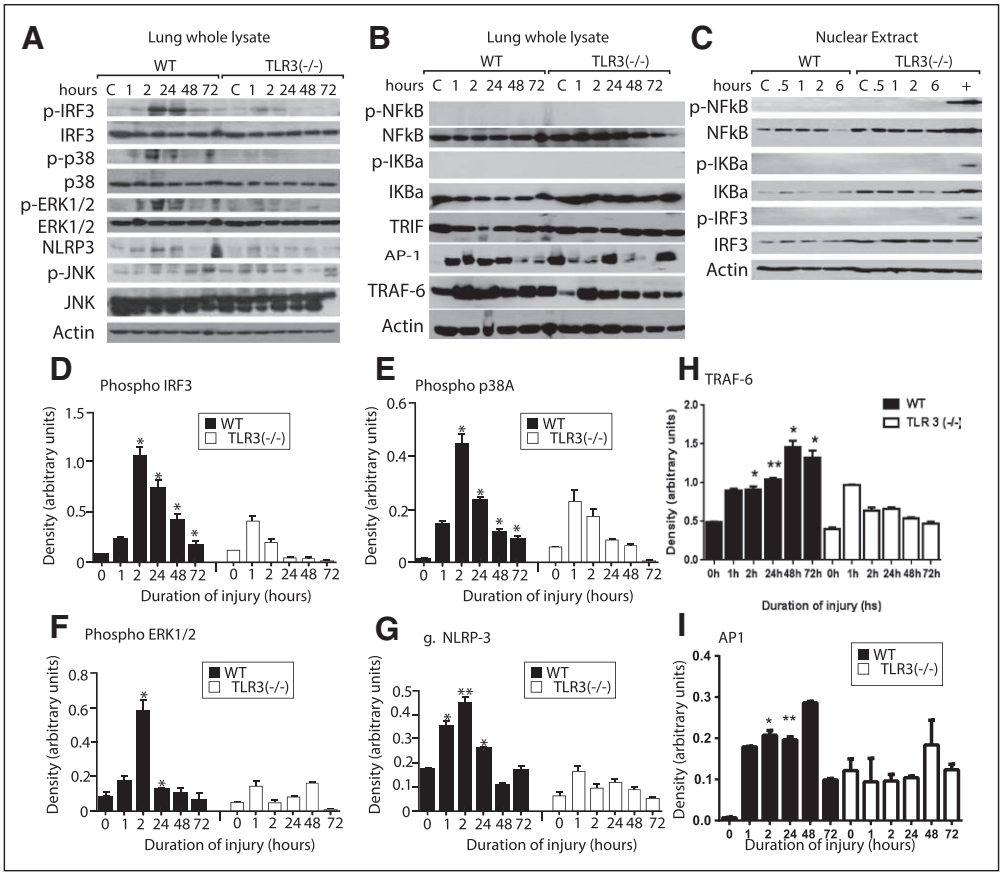

Figure 5. Toll-like receptor (TLR) 3/TIR-domain-containing adapter-inducing interferon-β (TRIF) pathway and downstream signaling activation following lung contusion (LC). Western blots. To determine TLR-3 downstream signaling activation following LC, lung lysates, and nuclear extracts were analyzed with Western blot using various antibodies ($n = 3$ per group). In whole lung lysate, phospho-interferon regulatory factor (IRF)-3, phospho-extracellular signal-regulated kinases (ERK) 1/2, and phospho-p38 mitrogen activated protein kinases (MAPK) were found to be reduced in TLR-3 (–/–) mice and no difference was found in phosphorylated JNK after LC (**A**). TLR-3 mice showed significant reductions in NOD-like receptor family pyrin domains-3 (NLRP-3) (**A**). Phosphorylated nuclear factor (NF)-κB and nuclear factor of NF-κB activation in whole lung lysate was not detected in WT or TLR-3 (–/–) mice after LC (**B**). Additionally, TRIF, TNF receptor-associated factor 6 (TRAF6), and activator protein (AP)-1 expression levels in whole lung lysate were not changed in WT or TLR-3. In nuclear extracts, phosphorylated NF-kB, IKBα, and IRF3 activation was not detected in WT or TLR-3 (–/–) mice following LC (**B**). In the nuclear extracts, phosphorylated NF-kB, IKBα, and IRF3 activation was not detected in WT or TLR-3 (–/–) mice after LC (**C**). Densitometry analyses of the proteins ($n = 3$) for each group were performed. *Error bars* indicate SEM. *$p < 0.05$ WT versus TLR-3 (–/–) (two-tailed *t* test).

with decreased production of proinflammatory cytokines, is characterized by an increased up-regulation of FIZZ-1/Arginine pathway and is indicative of the reparative process. The TLR-3 knockout mice exhibited a protective M2 as evidenced by increased Arginase-1 and Fizz-1 expression, suggestive of a functional alteration and change in polarity of AMs (**Fig. 4**, ***B*** and ***C***). There was significantly increased apoptosis at all-time points in the AMs from WT mice following LC compared with TLR-3 (–/–) mice (**Fig. 4*D***).

Surface Translocation of TLR-3 Increases Following LC. We performed experiments to evaluate whether there is surface translocation of TLR-3 with injury. Here, we used flow cytometry of macrophages to demonstrate that there is significant cell surface translocation of TLR-3 in WT mice following LC compared to the uninjured control (**Fig. 4*E***). These data indicate that LC has a significant impact on TLR-3 translocation.

Activation of MyD88 in Macrophages Following LC. Next, we sought to investigate whether the TLR-2/4 adaptor myeloid differentiation primary response gene 88 (MyD88), an activator of all TLRs, has the ability to modulate TLR-3 signaling following LC. Previous studies have shown an important role for TLR-4 and MyD88 in the evolution of acute inflammatory response following LC (20). We used flow cytometry of macrophages to demonstrate the expression of MyD88 in WT and TLR-3 (–/–) mice following LC. Our data showed that TLR-3 expression was significantly higher in WT mice, as expected, MyD88 expression was two-fold higher in TLR-3 (–/–) mice compared to the WT mice following LC (**Fig. 4*F***). In the absence of studies with dual knockout mice, this data suggest that the TLR-3/TRIF-induced inflammation and injury following LC is likely independent of complementary activation of pathways involving TLR-2 or 4.

Co-Culture of RNA From Necrotic Cells in the BAL With AMs. We next sought to determine whether the substances released by necrotic cells were responsible for the inflammatory response. KC, CCL5, and CCL3 were not activated upon addition of RNA from necrotic lung cells (neither at 100 ng nor at 1 μg/mL) in the TLR-3 (–/–) mice compared to WT mice (**Fig. 4*G***). The positive control in these experiments was the synthetic dsRNA molecule poly I:C. These data demonstrate that RNA from necrotic lung cells promotes an inflammatory response via the induction of potent proinflammatory mediators and thus represents the ligand for activation of TLR-3 in LC.

TLR-3/TRIF Pathway and Downstream Signaling Activation Following LC

Downstream Signaling in LC. To determine TLR-3 downstream signaling activation following LC, WT, and TLR-3 (–/–) mice, lung lysates and nuclear extracts were analyzed by Western blot using various antibodies (**Fig. 5*A***). While the WT lung lysates showed an increase in phospho-interferon (IFN) regulatory factor (IRF)-3, phospho-extracellular signal-regulated kinases 1/2,

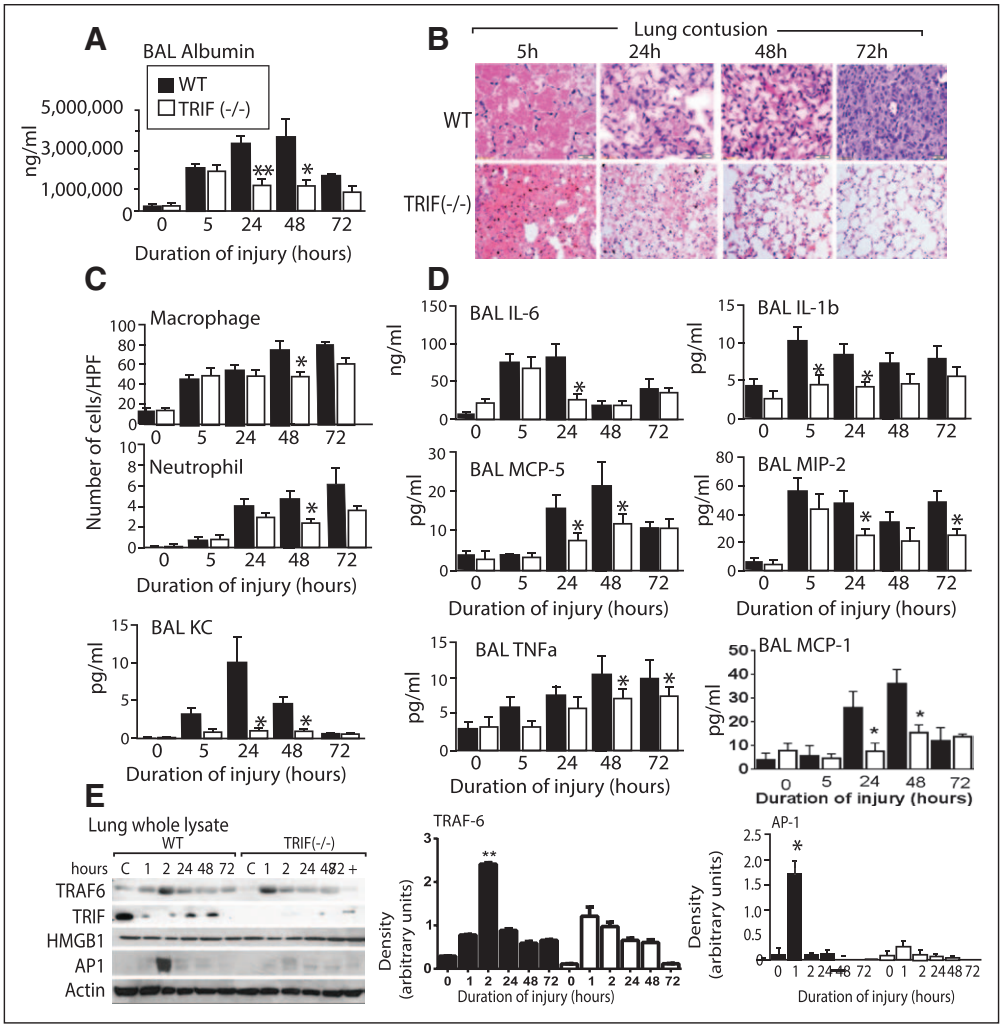

Figure 6. Functional importance of TIR-domain-containing adapter-inducing interferon-β (TRIF) in lung contusion (LC). **A**, Broncheoalveolar lavage (BAL) levels of albumin and cytokines: We performed separate experiments using TRIF (–/–) mice and corresponding wild-type (WT) mice and examined them at 5, 24, 48, and 72-hr time points. There was a significant increase in the BAL albumin level in WT mice. Values are represented as mean ($n = 12$–16 per group). $^{**}p < 0.01$ and $^{*}p < 0.05$ WT versus TRIF (–/–) mice. **B**, Histological evaluation of WT mice revealed significantly more inflammation, neutrophil infiltration, and wall edema at all-time points. **C**, Macrophage and neutrophil levels in BAL were lower in TRIF (–/–) mice following LC. There was a significant increase in the levels of macrophages and neutrophils in WT mice. **D**, TRIF (–/–) mice showed a significant reduction in cytokine response compared with WT following LC: The interleukin (IL)-6 levels in the BAL were significantly higher at 24 hr in WT mice following LC. The levels of IL-1β, monocyte chemotactic protein (MCP)-5, macrophage inflammatory protein (MIP)-2, keratinocyte chemoattractant (KC), and tumor necrosis factor (TNF)-α in the BAL were significantly decreased in TRIF (–/–) mice ($n = 12$). $^{*}p < 0.05$. **E**, TRIF downstream signaling activation following LC: The whole lung lysate extracts were analyzed with Western blot using various antibodies. TNF receptor-associated factor (TRAF) 6 and high-mobility group box 1 (HMGB1) expression did not vary between WT and toll-like receptor (TLR) 3. TLR-3 mice showed significant reductions in activator protein (AP)-1 expression at 2 hr compared with WT mice. Densitometry analyses of the proteins ($n = 3$ per group) for each group were performed. *Error bars* indicate SEM. $^{*}p < 0.05$ WT versus TRIF (–/–) (two-tailed *t* test). HPF = high power field.

and phospho-p38 mitrogen activated protein kinases (MAPK), an increased phosphorylation of IRF-3 was not observed in the nuclear isolates. Phosphorylated nuclear factor (NF)-κB and nuclear factor of NF-κB (IκBα) activation were not detected in WT or TLR-3 mice following LC. Additional immunofluorescence staining for phospho-NF-κB and total NF-κB revealed similar results (data not shown). TLR-3 (–/–) mice showed significant reductions in TNF receptor-associated factor 6 (**Fig. 5*B***) and NOD-like receptor family pyrin domains-3 (NLRP-3) compared to WT mice (Fig. 5*A*). The TLR-3/TRIF signaling pathway activation in LC is therefore independent of NF-κB and mediated through phosphorylation of p38 MAPK and ERK1/2. With significant differences in levels of IL-1β and IL-18 with NLRP-3, it thus appears that inflammasome activation independent of activation of NF-κb and IFN production is unique to TLR-3 mediated acute inflammation following LC (**Fig. 5**, *B* and ***C***).

TRIF Is Functionally Important in the Development of Progressive Lung Injury and Inflammation Following LC. We next evaluated the role of TRIF in LC. There was a significant increase in the BAL albumin level (**Fig. 6*A***) with histologic evidence of increased injury in WT mice at all-time points compared to TRIF (–/–) mice (**Fig. 6*B***). Similar results were observed with increased BAL cellularity (**Fig. 6*C***) and inflammatory cytokines (IL6, IL-1β, MCP-5, MIP-2, KC, and TNFα) (**Fig. 6*D***) in WT mice. These results suggest that TRIF plays an important role in upregulating the intensity of acute inflammation following LC.

In total, lung lysates and nuclear extracts phosphorylated NF-κB and IKBα activation were not detected in WT or TRIF (–/–) mice following LC (data not shown). TLR-3 mice showed significant reductions in activator protein (AP)-1 expression (**Fig. 6*E***). AP-1 is known to control a number of cellular processes including differentiation, proliferation, and apoptosis (22).

Role of dsRNA in Lung Inflammation Following LC

RNA Expression in WT Mice in BAL and Serum Samples Following LC. TLR-3 activation in viral diseases has been shown to be mediated specifically by ligation with dsRNA components from the infecting virus. However, what activates TLR-3 during acute inflammation secondary to LC is unclear. Using gel electrophoresis, we detected the presence of two

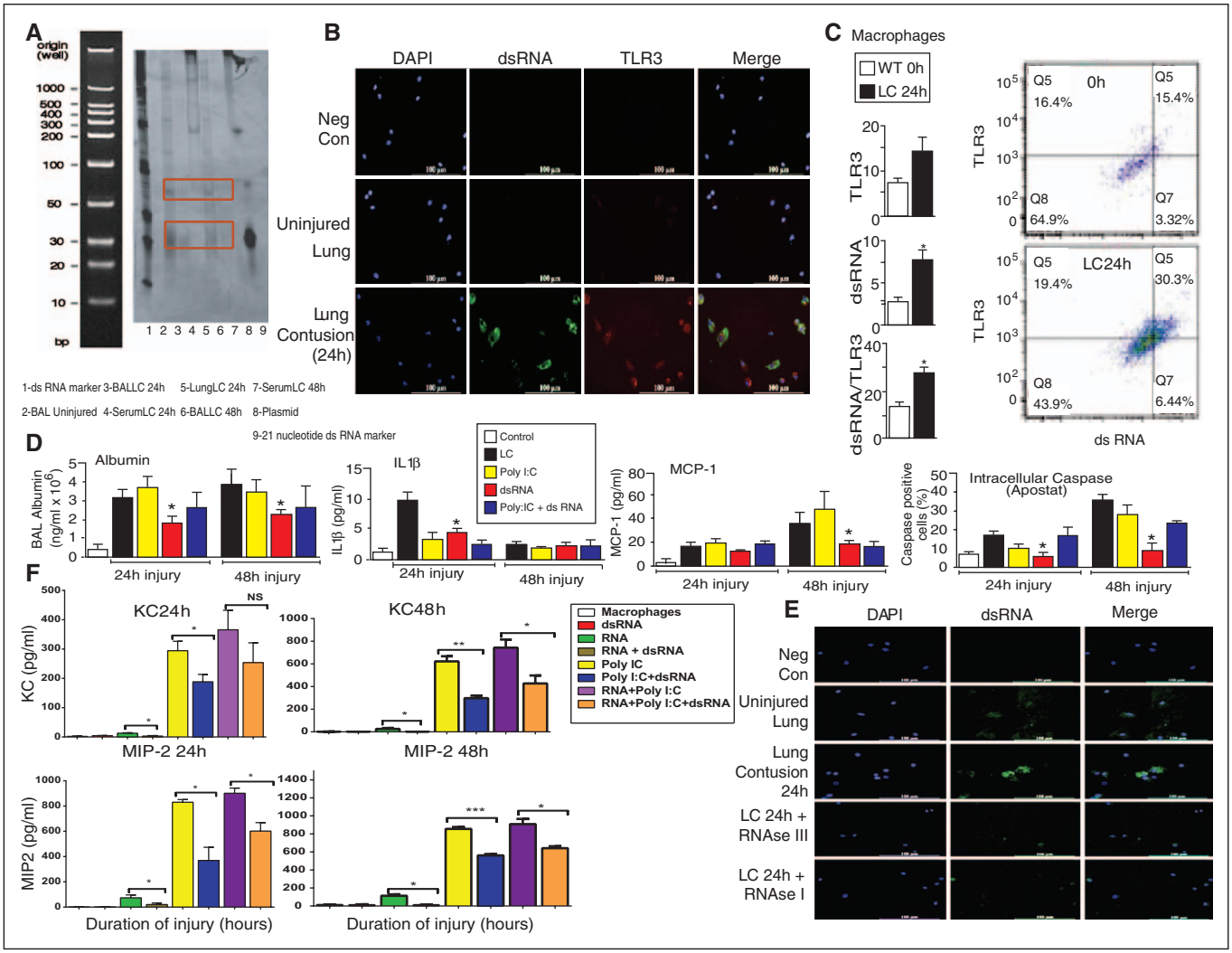

Figure 7. Increased double-stranded (ds) RNA release from injured cells is the ligand for the toll-like receptor (TLR) 3-driven acute inflammatory response following lung contusion (LC). **A**, dsRNA expression in wild-type (WT) mice in broncheoalveolar lavage (BAL) and serum samples following LC: Gel electrophoresis from BAL, lung, and serum samples in WT mice with and without LC. dsRNA bands were observed with BAL and serum samples (*red boxes*) following LC. **B**, Macrophages show elevated expression of dsRNA following LC. The macrophages from WT mice were harvested after LC and subjected to immunofluorescent staining with dsRNA (*green*), TLR-3 (*red*), and 4',6-diamidino-2-phenylindole (DAPI) (*blue*) ($n = 3$). **C**, dsRNA intracellular expression in BAL cells following LC. C57BL/6 mice were subjected to LC, and the levels of TLR-3 and dsRNA molecules on the cell surface were monitored by flow cytometry ($n = 3$). **D**, TLR-3/dsRNA complex inhibitor reduces injury and inflammation following LC. WT mice were administered the complex inhibitor 2 hr before LC, which significantly reduced the levels of albumin, cytokines (interleukin [IL]-1β and monocyte chemotactic protein [MCP]-1), and macrophage apoptosis. $^{*}p < 0.05$ dsRNA complex inhibitor versus LC alone. **E**, Effect of ribonuclease (RNAase) on dsRNA staining in macrophages following LC: After LC, macrophages were collected, fixed, permeabilized, and treated with 2 μg/mL of RNase III or 1 μg/mL of RNase A for 2 hr at 37°C. Cells were stained with antibody to dsRNA (*green*) and DAPI (*blue*) ($n = 3$). **F**, TLR-3/dsRNA complex inhibitor reduced the expression of proinflammatory cytokines by cultured macrophages following LC. Alveolar macrophages were cultured in the presence of RNA (obtained from the BAL cells of injured mice at 24 hr), and/or polyinosinic:polycytidylic acid (poly-I:C), RNA+ poly I:C with/without TLR-3/dsRNA inhibitor. The expression of proinflammatory cytokines was measured ($n = 4$). $^{***}p < 0.001$, $^{**}p < 0.01$, and $^{*}p < 0.05$ between corresponding groups in the presence/absence of dsRNA complex inhibitor. KC = keratinocyte chemoattractant, MIP = macrophage inflammatory protein.

distinct bands representing dsRNA of 20–30 and 30–50 base pairs in length in both cell-free BAL and serum from animals following LC (**Fig. 7*A***). Based on the number of base pairs, the shorter RNAs likely represent endogenous microRNAs and/or small interfering RNAs.

AM Show Increased Expression of dsRNA Following LC. Immunofluorescent imaging demonstrates intense dsRNA signal in AMs (J2 Ab [13]) from contused mice compared to corresponding uninjured controls (**Fig. 7*B***). Using flow cytometry, we observed a two-fold dsRNA and multi-fold TLR-3 expression increase with LC (**Fig. 7*C***). We found that dsRNA staining disappeared completely with RNase III treatment, a dsRNA-specific RNase, but only moderately with the preferably single-stranded RNA cleaving RNase A (23) (**Fig. 7*E***), supporting the notion that we are staining dsRNA.

TLR-3/dsRNA Complex Inhibitor Reduces the Injury and Inflammation Following LC. With the administration of TLR-3/dsRNA complex inhibitor (15) in the peritoneal cavity of animals prior to LC, there was a significant decrease in BAL albumin, total caspase activation in AMs (ApoStat), and

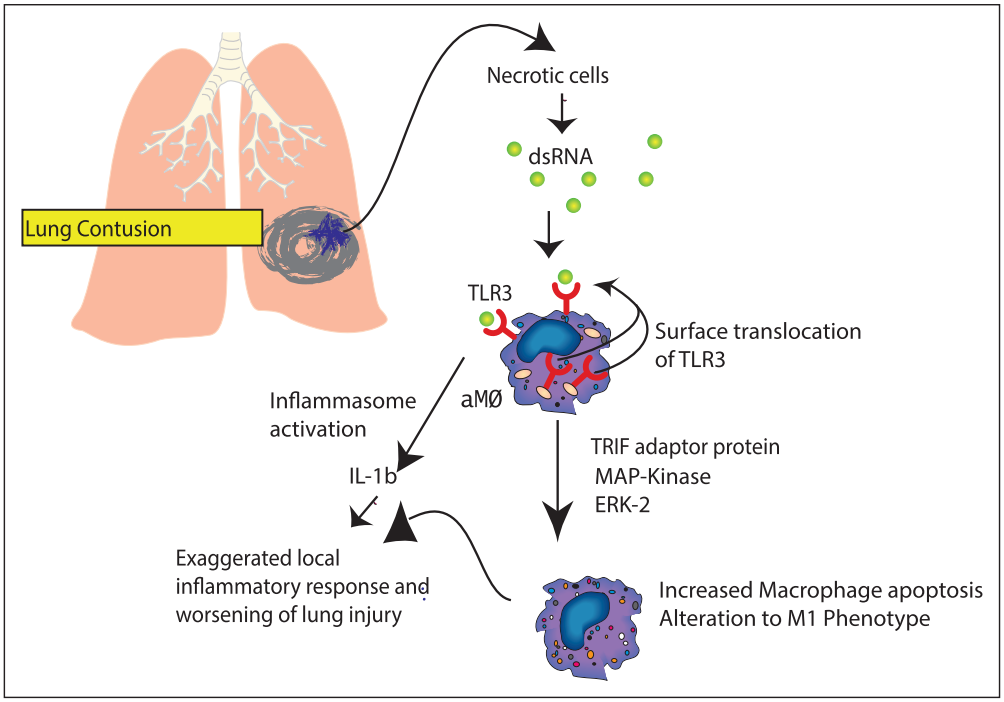

Figure 8. Proposed signal transduction pathways involving toll-like receptor (TLR) 3. Lung contusion (LC) induces alveolar disruption and cellular necrosis. Double-stranded (ds) RNA released from the cells are the key ligand for activation of the TLR-3, specifically located on the surface of the endosome. Additionally, the injury/inflammation causes a significant surface translocation of TLR-3, further amplifying the inflammatory process. The TLR-3/TIR-domain-containing adapter-inducing interferon-β (TRIF) signaling pathway activation in LC is independent of nuclear factor-κB and mediated through phosphorylation of p38 mitrogen activated protein kinases (MAPK) and extracellular signal-regulated kinases (ERK) 1/2. The major effect is borne on the alveolar macrophage inducing increased apoptosis and phenotypic alteration. TLR-3 recognition of dsRNA (Sjogren's Syndrome antibodies) also activates the inflammasome complex via (NOD-like receptor family pyrin domains-3, interleukin [IL] 1 β, IL18) to generate a robust proinflammatory response.

cytokine levels of IL-1β and MCP1 (**Fig. 7*D***). TLR-3/dsRNA complex inhibitor treatment significantly reduces the injury, inflammation, and apoptosis of the AMs following LC.

TLR-3/dsRNA Complex Inhibitor Attenuates the Expression of Proinflammatory Cytokines by Cultured Macrophages Ex-Vivo Following LC. AMs from WT injured/control mice were cultured in the presence of RNA obtained from BAL cells following LC, poly-I:C, and a combination of RNA and poly-I:C in the presence or absence of TLR-3/dsRNA complex inhibitor. RNA from the necrotic cells generated significantly higher expression in KC and MIP-2 at all the time points compared to control groups (**Fig. 7*F***). The TLR-3/dsRNA complex inhibitor significantly reduced proinflammatory cytokines levels in all groups. However, the ability of the inhibitor to reduce the activity of cytokine production with poly-I: C was limited. It is known that the activity of poly-I: C is also mediated through retinoic acid inducible gene-5 and malondialdehyde-5, two of the most important cytoplasmic sensors for activation of dsRNA (24, 25).

DISCUSSION

The major findings of our study confirm the importance of the TLR-3/TRIF pathway in the regulation of the acute inflammatory response in LC. Additionally, we report that dsRNA from injured cells is the ligand that interacts with TLR-3 in the context of inflammatory lung injury. There were major differences in the TLR-3 activation in LC when compared with the described dsRNA viral activation pathways. First, we observed translocation of the TLR-3 receptor to the surface of the AM following LC. Second, the downstream signaling is mediated through TRIF, ERK1/2, p38 MAPK, and AP-1, but is independent of NF-κB and does not involve type-1 interferon production. Additionally, the TLR-3 dependent activation of the inflammasome characterized by elevated levels of IL-1β, and IL-18 and NLRP-3 is independent of IFN or NF-κB activation (**Fig. 8**).

The major limitation of our study is the lack of relevant clinical data for the human lung samples that were subjected to immunohistochemistry. Though these patients had documented LC, it is not possible to confirm the precise nature and cause of death. It is entirely possible that these patients at the time of death had other serious illness including VAP and sepsis with multiple organ dysfunction. Additionally, a full characterization of the nature of the dsRNA was not performed.

In the previously reported swine model (26, 27), the insult is delivered by a captive bolt, and the animal is immediately placed on a mechanical ventilator. This places significant restrictions on the duration of the study but has its advantages in terms of easier instrumentation, such as study of cardiac output. In comparison, the murine model used in the current article, in addition to being a small animal model, has several advantages. We employ a spontaneously breathing mouse model following a closed-chest insult that eliminates the additional insult of ventilator-induced lung injury, the potential to be evaluated over a period of 7 days and provides ample opportunities to mechanistically study the pathways by the use of genetic knockouts and readily available primers/reagents.

In the present study, we found that LC is a potent trigger for the induction of TLR-3 expression in the lungs of both rodent and human samples. These changes are indicative of acute inflammation secondary to local mechanical trauma. These data indicate that AMs and epithelial cells are the primary cells involved in the activation of TLR-3 in LC. The major cell behind the TLR-3 driven acute inflammatory

response is the AM through its recruitment, activation, and phenotypic alteration. We show that in AMs following LC, there is increased surface translocation of TLR-3 and that this exposes the receptor to extracellular dsRNA released from injured cells. We note that recent data suggest that cigarette smoke augments the expression and response of TLR-3 in human macrophages, contributing to neutrophilic airway inflammation and parenchymal destruction in the lungs of smokers and patients with chronic obstructive pulmonary disease (COPD) (28).

Three distinct mechanisms explain the abrogated inflammatory response in the absence of TLR-3 in LC. One feature includes the reduction in apoptosis of the AM, a cell that plays a protective role in the resolution of inflammation (19), and this is a finding similar to observations in hyperoxia (29). The second mechanism involves the TLR-3 driven change in polarization of the macrophage. LC is known to promote increased recruitment of AMs to the site of injury (19). While a protective M2 phenotype is beneficial in LC (7). The M1 phenotype (also termed classically activated) is characterized by increased production of oxidative burst and nitric oxide release and secretion of proinflammatory cytokines (30). The significant increase in the levels of Arginase-1 and Fizz-1 in the TLR-3 (–/–) knockout genotype following LC demonstrate a protective M2 phenotype (alternatively activated), which is similar to (C-C) chemokine receptor (–/–) mice following LC (7). The M2 macrophage subpopulations may play a role in suppressing inflammation and initiating wound repair after acute injury (31).

Finally, we report that TLR-3 is an endogenous sensor of necrosis and that in its absence there is a reduction in the amplification of the inflammatory response following LC. The current work provides strong evidence that the dsRNA released from necrotic cells is the ligand for activation of TLR-3 in LC. This finding has significant therapeutic implications. Other TLRs (e.g., TLR-2/4) have been reported to play a role in the generation of acute inflammatory response following LC (20, 32). However, significant complications from uncontrolled Gram-positive and Gram-negative bacterial infections have been observed when the activities of these TLRs have been blocked (33–36). Currently, there are many agents available including monoclonal antibodies that have the ability to abrogate TLR-3 without any serious adverse effects. For example, monoclonal antibody from Innate Pharma that can bind to TLR3 (IPH33) is a monoclonal antibody targeting the TLR-3 receptor and it has been humanized (Innate Pharma, Marseille, France). Clinical use of these antibodies in COPD, rheumatoid arthritis, and inflammatory bowel disease have been proposed. Perturbation of this important sensing molecule and its downstream signaling pathways will therefore significantly increase our fundamental knowledge of and further inspire novel methods to restrict the inflammatory pathways associated with the exuberant local and systemic inflammatory activation associated with ARDS.

ACKNOWLEDGMENT

We thank Robin Kunkel for her help with the preparation of the article and figures.

REFERENCES

1. Cohn SM: Pulmonary contusion: Review of the clinical entity. *J Trauma* 1997; 42:973–979
2. Miller PR, Croce MA, Bee TK, et al: ARDS after pulmonary contusion: Accurate measurement of contusion volume identifies high-risk patients. *J Trauma* 2001; 51:223–228; discussion 229–230
3. Tsujimoto H, Ono S, Efron PA, et al: Role of Toll-like receptors in the development of sepsis. *Shock* 2008; 29:315–321
4. Alexopoulou L, Holt AC, Medzhitov R, et al: Recognition of double-stranded RNA and activation of NF-kappaB by Toll-like receptor 3. *Nature* 2001; 413:732–738
5. Brentano F, Schorr O, Gay RE, et al: RNA released from necrotic synovial fluid cells activates rheumatoid arthritis synovial fibroblasts via Toll-like receptor 3. *Arthritis Rheum* 2005; 52:2656–2665
6. Karikó K, Ni H, Capodici J, et al: mRNA is an endogenous ligand for Toll-like receptor 3. *J Biol Chem* 2004; 279:12542–12550
7. Suresh MV, Yu B, Machado-Aranda D, et al: Role of macrophage chemoattractant protein 1 in acute inflammation following lung contusion. *Am J Respir Cell Mol Biol* 2012; 46:797–806
8. Dolgachev VA, Yu B, Reinke JM, et al: Host susceptibility to gram-negative pneumonia after lung contusion. *J Trauma Acute Care Surg* 2012; 72:614–622
9. Benias PC, Gopal K, Bodenheimer H Jr, et al: Hepatic expression of toll-like receptors 3, 4, and 9 in primary biliary cirrhosis and chronic hepatitis C. *Clin Res Hepatol Gastroenterol* 2012; 36:448–454
10. Chuang JH, Chuang HC, Huang CC, et al: Differential toll-like receptor 3 (TLR3) expression and apoptotic response to TLR3 agonist in human neuroblastoma cells. *J Biomed Sci* 2011; 18:65
11. Jorgenson RL, Young SL, Lesmeister MJ, et al: Human endometrial epithelial cells cyclically express Toll-like receptor 3 (TLR3) and exhibit TLR3-dependent responses to dsRNA. *Hum Immunol* 2005; 66:469–482
12. Suresh MV, Ramakrishnan SK, Thomas B, et al: Activation of hypoxia-inducible factor-1α in type 2 alveolar epithelial cell is a major driver of acute inflammation following lung contusion. *Crit Care Med* 2014; 42:e642–e653
13. Miorin L, Albornoz A, Baba MM, et al: Formation of membrane-defined compartments by tick-borne encephalitis virus contributes to the early delay in interferon signaling. *Virus Res* 2012; 163:660–666
14. Bauhofer O, Summerfield A, McCullough KC, et al: Role of double-stranded RNA and Npro of classical swine fever virus in the activation of monocyte-derived dendritic cells. *Virology* 2005; 343:93–105
15. Takemura N, Kawasaki T, Kunisawa J, et al: Blockade of TLR3 protects mice from lethal radiation-induced gastrointestinal syndrome. *Nat Commun* 2014; 5:3492
16. Raghavendran K, Davidson BA, Helinski JD, et al: A rat model for isolated bilateral lung contusion from blunt chest trauma. *Anesth Analg* 2005; 101:1482–1489
17. Raghavendran K, Davinnnnnnbvdson BA, Huebschmann JC, et al: Superimposed gastric aspiration increases the severity of inflammation and permeability injury in a rat model of lung contusion. *J Surg Res* 2009; 155:273–282
18. Raghavendran K, Notter RH, Davidson BA, et al: Lung contusion: Inflammatory mechanisms and interaction with other injuries. *Shock* 2009; 32:122–130
19. Machado-Aranda D, V Suresh M, Yu B, et al: Alveolar macrophage depletion increases the severity of acute inflammation following nonlethal unilateral lung contusion in mice. *J Trauma Acute Care Surg* 2014; 76:982–990
20. Hoth JJ, Wells JD, Brownlee NA, et al: Toll-Like receptor 4 dependent responses to lung injury in a murine model of pulmonary contusion. *Shock* 2009; 31:376–381

21. Johnston LK, Rims CR, Gill SE, et al: Pulmonary macrophage subpopulations in the induction and resolution of acute lung injury. *Am J Respir Cell Mol Biol* 2012; 47:417–426
22. Hess J, Angel P, Schorpp-Kistner M: AP-1 subunits: Quarrel and harmony among siblings. *J Cell Sci* 2004; 117:5965–5973
23. Rojas M, Arias CF, López S: Protein kinase R is responsible for the phosphorylation of eIF2alpha in rotavirus infection. *J Virol* 2010; 84:10457–10466
24. Gitlin L, Barchet W, Gilfillan S, et al: Essential role of mda-5 in type I IFN responses to polyriboinosinic: Polyribocytidylic acid and encephalomyocarditis picornavirus. *Proc Natl Acad Sci U S A* 2006; 103:8459–8464
25. Yoneyama M, Kikuchi M, Matsumoto K, et al: Shared and unique functions of the DExD/H-box helicases RIG-I, MDA5, and LGP2 in antiviral innate immunity. *J Immunol* 2005; 175:2851–2858
26. Davis KA, Fabian TC, Croce MA, et al: Prostanoids: Early mediators in the secondary injury that develops after unilateral pulmonary contusion. *J Trauma* 1999; 46:824–831
27. Davis KA, Fabian TC, Ragsdale DN, et al: Endogenous adenosine and secondary injury after chest trauma. *J Trauma* 2000; 49:892–898
28. Koarai A, Yanagisawa S, Sugiura H, et al: Cigarette smoke augments the expression and responses of toll-like receptor 3 in human macrophages. *Respirology* 2012; 17:1018–1025
29. Murray LA, Knight DA, McAlonan L, et al: Deleterious role of TLR3 during hyperoxia-induced acute lung injury. *Am J Respir Crit Care Med* 2008; 178:1227–1237
30. Trujillo G, O'Connor EC, Kunkel SL, et al: A novel mechanism for CCR4 in the regulation of macrophage activation in bleomycin-induced pulmonary fibrosis. *Am J Pathol* 2008; 172:1209–1221
31. Byers DE, Holtzman MJ: Alternatively activated macrophages and airway disease. *Chest* 2011; 140:768–774
32. Hoth JJ, Hudson WP, Brownlee NA, et al: Toll-like receptor 2 participates in the response to lung injury in a murine model of pulmonary contusion. *Shock* 2007; 28:447–452
33. O'Brien AD, Rosenstreich DL, Scher I, et al: Genetic control of susceptibility to Salmonella typhimurium in mice: Role of the LPS gene. *J Immunol* 1980; 124:20–24
34. O'Neill LA, Bryant CE, Doyle SL: Therapeutic targeting of Toll-like receptors for infectious and inflammatory diseases and cancer. *Pharmacol Rev* 2009; 61:177–197
35. Weiss DS, Raupach B, Takeda K, et al: Toll-like receptors are temporally involved in host defense. *J Immunol* 2004; 172:4463–4469
36. Weiss DS, Takeda K, Akira S, et al: MyD88, but not toll-like receptors 4 and 2, is required for efficient clearance of *Brucella abortus*. *Infect Immun* 2005; 73:5137–5143